




Article

A Novel Hybrid Die Design for Enhanced Grain Refinement: Vortex Extrusion–Equal-Channel Angular Pressing (Vo-CAP)

Hüseyin Beytüt ^{1,*} , Kerim Özbeyaz ¹  and Şemsettin Temiz ² ¹ Department of Faculty of Engineering and Architecture, Bitlis Eren University, 13000 Bitlis, Türkiye; kozbeyaz@beu.edu.tr² Department of Faculty of Engineering, İnönü University, 44100 Malatya, Türkiye; semsettin.temiz@inonu.edu.tr

* Correspondence: hbeytut@beu.edu.tr

Abstract: A novel hybrid Severe Plastic Deformation (SPD) method called Vortex Extrusion–Equal-Channel Angular Pressing (Vo-CAP) was developed and applied to AA6082 workpieces in this study. Before experimental application, a comprehensive optimization of the die design was performed considering effective strain, strain inhomogeneity, and pressing load parameters. The optimization process utilized an integrated approach combining Finite Element Analysis (FEA), artificial neural networks (ANNs), and the non-dominated sorting genetic algorithm II (NSGA-II). The optimized die successfully achieved a balance between maximizing effective strain while minimizing pressing load and strain inhomogeneity. The Vo-CAP process incorporates a unique conical die design that enables assembly without traditional fasteners. Moreover, this novel die combines VE and ECAP advantages in a single-pass operation. While VE has been previously studied, experimental work was limited to specific configurations, and its integration with ECAP had not been explored. Through the development of Vo-CAP, this research gap has been addressed. The results showed substantial enhancements in hardness values, ultimate tensile strength, and strain homogeneity. These findings demonstrate that Vo-CAP represents a significant advancement in SPD, offering an efficient single-pass process for improving the mechanical properties of aluminum alloys through grain refinement.

Keywords: severe plastic deformation (SPD); equal channel angular pressing (ECAP); vortex extrusion; AA6082; die design optimization; finite element analysis (FEA)



Academic Editor: Myoung-Gyu Lee

Received: 8 November 2024

Revised: 28 December 2024

Accepted: 29 December 2024

Published: 2 January 2025

Citation: Beytüt, H.; Özbeyaz, K.; Temiz, Ş. A Novel Hybrid Die Design for Enhanced Grain Refinement: Vortex Extrusion–Equal-Channel Angular Pressing (Vo-CAP). *Appl. Sci.* **2025**, *15*, 359. <https://doi.org/10.3390/app15010359>

Copyright: © 2025 by the authors. Licensee MDPI, Basel, Switzerland. This article is an open access article distributed under the terms and conditions of the Creative Commons Attribution (CC BY) license (<https://creativecommons.org/licenses/by/4.0/>).

1. Introduction

The metalworking industry has always aimed to enhance the mechanical properties of metals, focusing on hardness, strength, and ductility, which are crucial properties for engineering applications. Severe Plastic Deformation (SPD) has become a key technique for achieving this goal. SPD processes apply high levels of strain to the metals without changing their volume significantly. This process initiates grain refinement, which reduces the average size of the grains in the metal and results in an Ultra-Fine Grain (UFG) structure. As a result, the mechanical properties of the materials enhances [1,2]. The Hall–Petch relation, a basic concept in metallurgy, supports this improvement by indicating that the strength of a material is inversely proportional to its grain size. In other words, smaller grains lead to stronger materials [3,4]. This principle demonstrates the potential of SPD applications in material science, driving continued research and interest in these field.

Over the past three decades, a variety of SPD methods have been developed and implemented. Each has been designed to optimize grain refinement, improve mechanical

properties, and reduce processing times. Well-established methods include Equal-Channel Angular Pressing (ECAP), where a metal billet is pressed through a sharply angled die channel, refining the grain structure and increasing the strength of the materials [5–8]. One other SPD method is Twist Extrusion (TE), involving the twisting of a metal billet through a die channel to produce high strain without significant dimensional changes [9,10]. Another well-known SPD method is High-Pressure Torsion (HPT), which uses high pressure to twist a metal workpiece, creating highly uniform, refined grains for better mechanical properties [11,12]. Accumulative Roll-Bonding (ARB) is one of the famous SPD methods, which is a simpler method that is easier to scale and stacks, rolls, and sections thin metal sheets repeatedly, progressively refining their grain structure [13,14].

Despite the examples of SPD methods mentioned above, researchers continue to develop new techniques to achieve further grain refinement, to create more uniform microstructures, and to reduce the processing time for greater efficiency. When the literature is examined in more detail based on the efficiency of the SPD techniques, ECAP remains one of the most commonly used techniques due to its simplicity and efficient process, which significantly enhances the mechanical properties of materials by obtaining UFG structures. However, achieving the desired mechanical properties and homogeneity often requires multiple processing iterations, called passes, extending process durations. To address these challenges, researchers have developed several modifications based on the ECAP method by integrating new die designs. Some of these modifications include C-ECAP (Conform ECAP) [15–17], ECAP-BP (ECAP with Back Pressure) [18,19], RD-ECAP (Rotary-die ECAP) [20], I-ECAP (Incremental ECAP) [21], and Exp.-ECAP (Expansion Equal-Channel Angular Pressing) [22].

Apart from classical SPD techniques, in recent years, researchers have developed new extrusion-based techniques to produce UFG structures and enhance the mechanical properties of materials. Some of these techniques include Twist Extrusion (TE) [9,10], Vortex Extrusion [23–26], Simple Shear Extrusion (SSE) [27,28], Equal-Channel Forward Extrusion (ECFE) [29,30], Repetitive Upsetting Extrusion (RUE) [31,32], Gradation Extrusion (GE) [33,34], and Thin-Walled Open-Channel Angular Pressing (TWO-CAP) [35–37]. Among these methods, one of the most interesting methods is Vortex Extrusion (VE), which was introduced by Shahbaz et al. in 2011 as a new extrusion-based SPD technique. In this method, the material passes through a specially designed ‘vortex zone’ that induces rotational motion [24]. A subsequent study explored the material flow and mathematical modeling of the vortex zone [23]. Moreover, research identified the twist angle, the twist zone length, and the reduction area as critical optimization variables to maximize process efficiency and minimize pressing load [26]. However, a detailed literature review revealed that experimental work on VE has so far been limited to a specific configuration with a 60° twist angle and 10 mm vortex zone length [25].

To enhance the efficiency of classical SPD processes, another procedure involves integrating the various SPD techniques into a single die, referred to as hybrid or combined SPD techniques. In general, a hybrid die combines multiple SPD techniques into a single die, allowing for simultaneous pressing of the material. This approach merges the advantages of two or more SPD methods, resulting in a product with significantly improved homogeneity and enhanced mechanical properties. Some of these combined SPD techniques are the following: twist channel angular pressing (ECAP + TE); TE and ECAP processes have been integrated into a single die [38]. Forward extrusion ECAP (FE-ECAP) combines extrusion and ECAP in a single die [39,40], TV-CAP (Twisted Variable Channel Angular Pressing) consists of adding a twist and extrusion zones to the classic ECAP die channels [9,10].

Aluminum alloys such as AA6082 have proven to be a popular choice in SPD studies due to their favorable mechanical properties and response to grain refinement processes.

Researchers have extensively explored the alloy AA6082 in various SPD methods, establishing its significance in material science. Khelfa et al. (2019) demonstrated that ECAP under warm conditions led to refined grain structure and increased strength in AA6082; although, softening occurred after multiple passes [41]. Baig et al. (2016) focused on the combined effect of ECAP and aging, achieving substantial improvements in yield strength and hardness [42]. Balasubramanian et al. (2021) explored the ECAP bonding process with AA6082 and MgAZ31B, revealing challenges in dissimilar material bonding due to differences in ductility and emphasized the importance of route selection and die design in optimizing mechanical properties [43].

Although a variety of techniques exist, as mentioned in the details above, further refinement and modernization are required for wider applications. When the literature is examined as mentioned above, it is seen that one of the attractive SPD methods is VE. And due to the limited optimization and experimental studies on VE in the literature, it is believed that more comprehensive optimization research is necessary to increase the technique's efficiency. Hence, this paper aims to achieve significant advancements in the field by introducing a novel die design called Vortex Extrusion–Equal-Channel Angular Pressing (Vo-CAP). This novel die combines VE and ECAP into one unified system to harness the advantages of both methods. In order to achieve this goal, the first step was to model the Vo-CAP die and carry out a Finite Element Analysis (FEA) using the DEFORM-3D software (Version 11.0). The obtained results were compared with the literature, and the efficiency and applicability of this novel method was investigated. Later on, to enhance the process efficiency, specific design variables were optimized. The optimized die was manufactured, and the AA6082 material was used as workpiece material. Furthermore, hardness and tensile mechanical tests were carried out to examine the mechanical properties and were compared with annealed workpieces and the literature. Moreover, microstructural analysis was conducted by Optic Microscope (OM) images.

2. Materials and Method

The processes in this study were carried out in multiple stages to comprehensively analyze the Vo-CAP process and its effect on AA6082. The approach included material preparation, die design, die channel optimization, finite element modeling (FEM), experimental validation, mechanical tests, and microstructural investigation. The die design was optimized using a combination of FEA and optimization methods. Subsequently, experiments were conducted using the optimized die to process the AA6082 workpiece. Finally, the mechanical properties and microstructural changes in the processed material were investigated. The following sections provide detailed descriptions of each stage.

2.1. Materials

2.1.1. Workpiece Material

The workpiece material used in this study was AA6082. The as-received alloy was in the form of extruded rods with a diameter of 20 mm. The chemical composition of the alloy studied in this study is presented in Table 1.

Table 1. Chemical composition of AA6082 (EN AW 6082).

Elements	Si	Mg	Mn	Fe	Cr	Cu	Zn	Al
Weight (%)	1.2	0.78	0.5	0.3	0.14	0.08	0.05	balance

Prior to SPD processing, the extruded rods were machined into cylindrical billets with a length of 40 mm while maintaining the original diameter of 20 mm. To ensure a

homogeneous starting microstructure and remove any potential segregations, residual stresses, or inhomogeneities from the as-received condition, the billets were subjected to a homogenization heat treatment. This treatment was carried out using a Protherm PLF110/10 chamber furnace in Bitlis Eren University. The workpieces were heated to 460 °C and held at this temperature for 3 h and cooled to room temperature by air.

2.1.2. Die and Other Components Materials

Due to the processing temperature of 210 °C, materials capable of withstanding high temperatures were selected for the die, the die holders, and the other fixing apparatus. The chosen material for the die is AISI P20 Impax Supreme, which is characterized by its exceptional hardness, wear resistance, and stability at elevated temperatures. To achieve precision in the die's vortex zone, a five-axis CNC machine was employed for its manufacturing. Following the completion of the die, a hardening process was applied to elevate its hardness level to 56 HRC, ensuring enhanced durability during the SPD process. Additionally, AISI H13 (DIN 1.2344) steel, which offers excellent thermal resistance and mechanical strength, was used to fabricate the die holder, punch component, and all other fixing apparatus.

2.2. Die Design

The Vo-CAP hybrid die features an innovative and integrated design, characterized by the right and left die components and the die holder being shaped conically as shown in Figure 1. This conical geometry not only facilitates the integration of components without the need for fasteners such as bolts and nuts but also allows for easy removal and separation of the dies after the Vo-CAP process. This dual-purpose conical design thus enhances the overall efficiency of both the assembly and disassembly processes. Furthermore, the exit channel is slightly sloped as shown with the red dashed lines in Figure 1a to keep the material aligned after pressing.

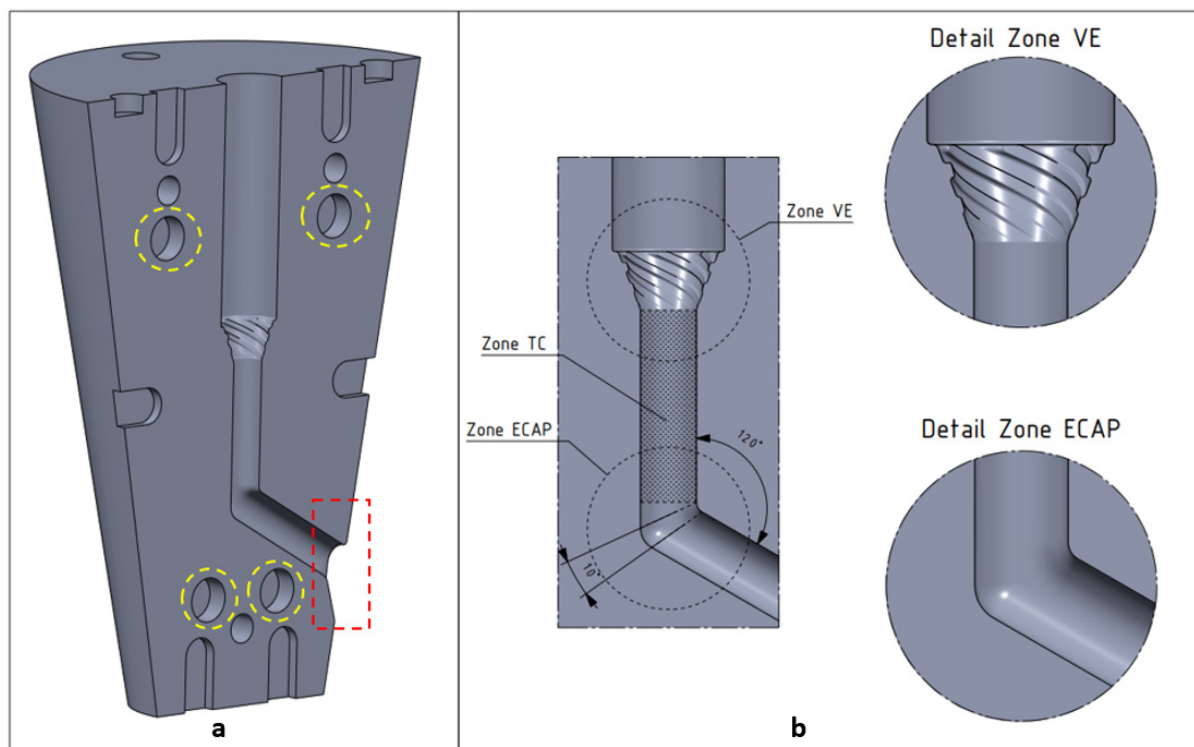


Figure 1. Design of novel Vo-CAP die. (a) 3D view of the die. (b) Detailed view of the zones (VE and ECAP).

As shown in Figure 1a, channels for four pin holes illustrated with yellow circles have been incorporated into the die holder to secure the die during the process and to maintain synchronized movement between the right and left die components. This design feature helps to prevent any unwanted movement and provides stability during the pressing operation.

The hybrid die consists of three main zones, as illustrated in Figure 1b. The first zone, known as the Vortex Extrusion (VE) zone, introduces torsional deformation to the material. The second zone, the Transition Channel (TC) zone, connects the VE and ECAP zones, thereby ensuring the continuity of deformation. The third zone, the Equal-Channel Angular Pressing (ECAP) zone, imposes severe shear deformation to refine the material grains. This zone features an inner angle (Φ) of 120° and an outer corner angle (Ψ) of 10° .

2.3. Finite Element Analysis (FEA)

In this study, the DEFORM 3D (Version 11.0) software was employed to conduct a FEA to simulate the Vo-CAP process. The simulation setup, as illustrated in Figure 2, consisted of four main components: the workpiece, punch, die, and die holder. The workpiece was modeled as a deformable body using AA6082 material properties, with a diameter of 20 mm and a length of 40 mm. Importantly, the workpiece temperature was maintained at a constant 210°C throughout the analysis, simulating isothermal processing conditions.

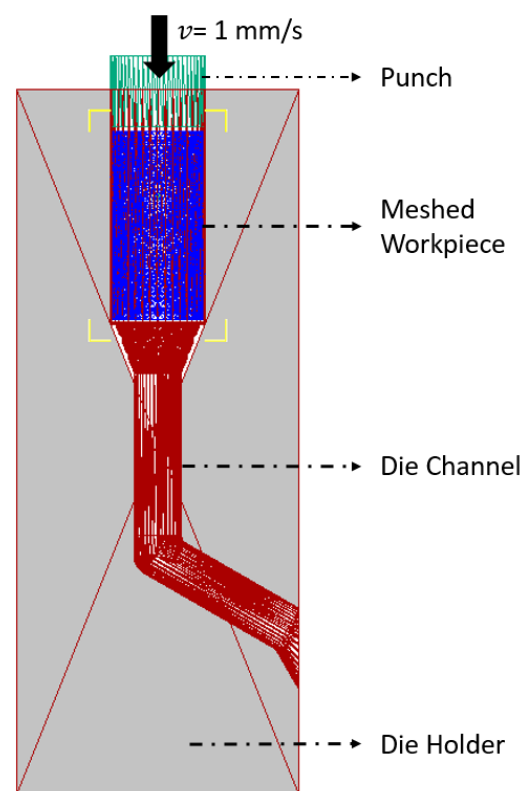


Figure 2. FEM setup of Vo-CAP.

Based on the mesh convergence study, the workpiece was meshed with 60,000 tetrahedral elements, which provided optimal accuracy for strain and stress calculations while maintaining computational efficiency. Furthermore, to account for substantial deformations during the analysis, an automatic re-meshing technique was implemented.

The punch and die were modeled as rigid bodies to simplify the computational requirements while accurately capturing the deformation behavior of the workpiece. This approach allows the software to focus on the material flow and strain distribution within

the deformable workpiece. A critical aspect of the simulation was the interface between the workpiece and die. The shear coefficient of friction was determined to be 0.1, a finding that was arrived at through a comprehensive review of the extant literature, a rigorous testing program of lubricants conducted within an experimental environment, and a detailed analysis of the catalog values of lubricants, and the punch velocity was set at 1 mm s^{-1} . The objective was to press at the slowest possible speed, despite the fact that, in theory, this parameter does not appear to be effective in the process, given its impact on the recovery process during material flow. In addition, the punch movement was constrained in all directions except for its motion axis, providing stability during the pressing process.

The die stroke was set as a control parameter, with appropriate stopping controls to define the process limits. To stop the simulation, the value of the stroke was set to be equal to the length of the workpiece, i.e., 40 mm. Thanks to this comprehensive setup, an accurate modeling and analysis of the Vo-CAP process under hot forming conditions has been made possible.

The FEM model used in the present study has been validated by comparison with the study carried out by Shahbaz et al. [24]. In this context, the same material (AA1050) and same process parameters were applied and resimulated. The obtained effective strain and highest pressing load results were compared for validation.

2.4. Optimization of Die Design

For SPD methods, the die design is crucial in improving the mechanical properties of materials as mentioned above. For this reason, many studies have focused on the design and optimization of dies to increase process efficiency and to further improve and enhance the properties of the materials at the end of the process [26,44,45]. For these reasons, the following optimization studies were performed as a novel and significant part of this study. The framework of the optimization is given in Figure 3.

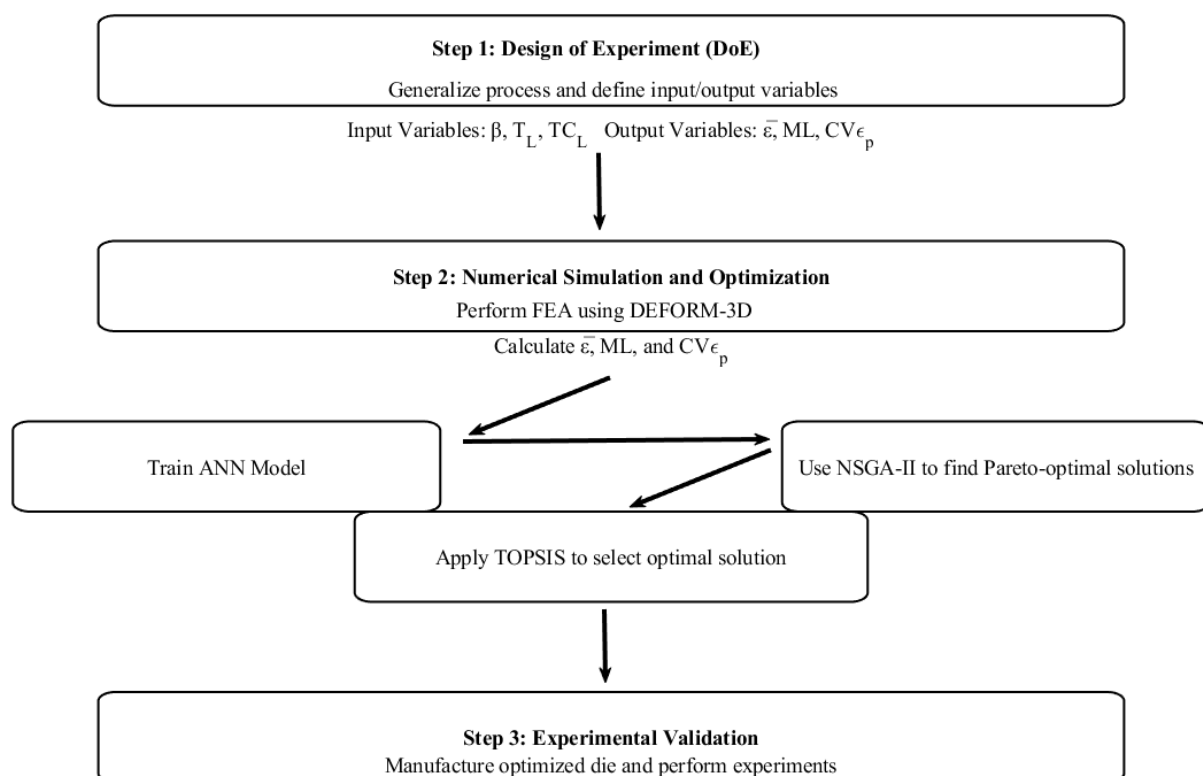


Figure 3. Optimization framework for Vo-CAP.

Initially, a Design of Experiments (DoEs) approach was implemented to establish a design space. After building a dataset, an integrated optimization approach combining artificial neural networks (ANNs) and the non-dominated sorting genetic algorithm II (NSGA-II) was developed. The ANN was trained to predict die performance based on the design parameters, while the NSGA-II was employed to find Pareto-optimal solutions that maximize the effective strain while minimizing the pressing load and the strain inhomogeneity.

To determine the most optimal solution from the Pareto set generated by the NSGA-II, the Technique for Order of Preference by Similarity to Ideal Solution (TOPSIS) method was applied [46]. This multi-criteria decision making (MCDM) technique made it possible to balance the trade-offs between the objectives of this study and to select the die design parameters that best met all the criteria at the same time. This systematic approach, combining DoE, FEM, ANN, NSGA-II, and TOPSIS, enabled the design space to be efficiently explored and the optimal die configuration for the Vo-CAP process to be identified.

2.4.1. Optimization Objectives

In this study, effective strain ($\bar{\epsilon}$), strain inhomogeneity ($CV_{\epsilon p}$), and maximum pressing load (ML) were considered as optimization objectives. These parameters play a crucial role in enhancing the mechanical properties of the material and improving the overall effectiveness of the process. High effective strain values correspond to improved mechanical properties. Therefore, numerous studies, both in the past and present, have been conducted to increase effective strain [8,47–49]. Strain inhomogeneity, on the other hand, plays a critical role in assessing the effectiveness of SPD processes. Consequently, numerous studies have been conducted by researchers in recent years to evaluate strain inhomogeneity [50–52]. Strain inhomogeneity is measured by dividing the standard deviation of the effective strain values by the average effective strain value and is called the Coefficient of Inhomogeneity ($CV_{\epsilon p}$). The formula for calculating $CV_{\epsilon p}$ is given as follows [53]:

$$CV_{\epsilon p} = \frac{Stdev_{\epsilon p}}{Av_{\epsilon p}}$$

This coefficient provides a normalized measurement to assess the level of strain inhomogeneity by relating the variability of strain values to their mean, which is crucial in optimization studies focused on improving the uniformity of material deformation. After the FEM analysis, to find the $CV_{\epsilon p}$, 72 points were chosen across the cross-sectional plane of the workpiece as seen in Figure 4. Thanks to the DEFORM 3D (V11.0) software, the effective strain values at these points were extracted and evaluated to determine how evenly the effective strain was distributed throughout the material.

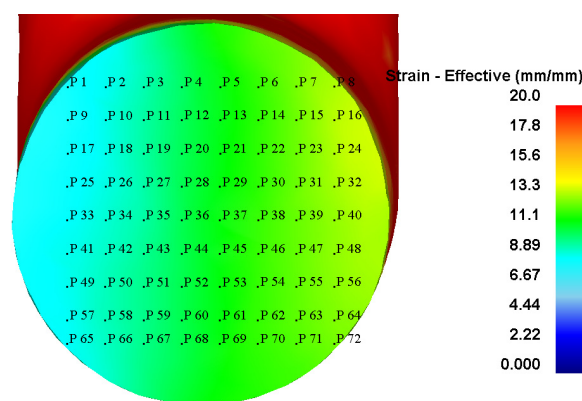


Figure 4. Selected point across the cross-sectional plane.

Pressing load represents the amount of force applied to the workpiece during the deformation process. Although achieving high effective strain and homogeneity are key objectives, it is equally important to minimize the pressing load. High pressing loads can result in several undesirable consequences, such as increased energy consumption, higher tool wear, and potential damage to the die or workpiece. To address these challenges and improve process efficiency, numerous studies in recent years have focused on minimizing the pressing load [22,26]. After the FEAs, the stroke-force graphs of the process were extracted and recorded.

2.4.2. Design of Experiments

To systematically examine the impact of Vo-CAP die parameters on key objectives, a DoEs approach was employed. In this study, three critical design variables were focused on: twist angle (β), twist length (T_L), and Transition Channel Length (TC_L). These design parameters are illustrated in Figure 5. For each parameter, lower and upper values were defined, which are presented in Table 2. By varying these parameters, 27 unique die designs were generated. Each design was then analyzed using FEM to determine the effective strain, maximum pressing load, and strain inhomogeneity values. Then, this dataset was used for the optimization process.

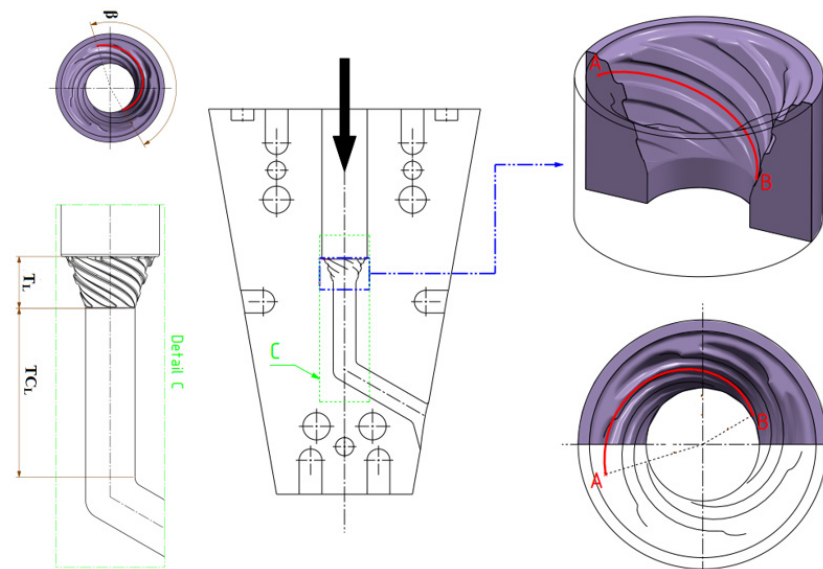


Figure 5. Geometric representation of variables.

Table 2. Design variables and their bonds.

Design Variables	Range	Unit	Symbol
Twist angle	$[30^\circ-180^\circ]$	$^\circ$	β
Twist length	$[10-40]$	mm	T_L
Transition Channel Length	$[10-50]$	mm	TC_L

2.4.3. Artificial Neural Network (ANN)

An ANN was used to model the relationship between input parameters and output responses. ANNs are known for their ability to model complex nonlinear relationships and have been widely used in various engineering applications [54,55]. The network had three layers: an input layer with 3 neurons, a hidden layer with 15 neurons, and an output layer with 3 neurons, as illustrated Figure 6. The Levenberg–Marquardt algorithm was used for training ANNs due to its efficiency and robustness [56]. The dataset was divided into training (70%), validation (15%), and testing (15%) subsets. To manage data variability,

each data point was normalized within a range of 0 to 1. The mean squared error (MSE) was used to evaluate the network's accuracy.

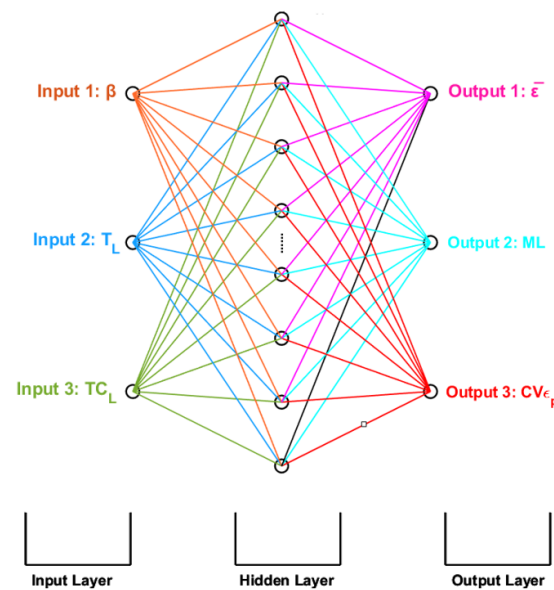


Figure 6. Basic structure of the implemented ANN model.

2.4.4. Non-Dominated Sorting Genetic Algorithm II (NSGA-II)

After obtaining the best-performing ANN models, a multi-objective optimization was performed using the NSGA-II to find Pareto-optimal solutions. The NSGA II is a multi-objective evolutionary algorithm used to optimize problems with conflicting objectives. The NSGA-II aims to find a set of Pareto-optimal solutions, where no one solution is strictly better than another in all objectives [57]. The optimization aimed to maximize effective strain while minimizing pressing load and strain inhomogeneity by varying the input parameters within their ranges, as specified in Table 2.

In the NSGA-II optimization, population size and generations were set at 100 to allow sufficient exploration of the solution space. A crossover fraction of 0.7 was set to promote diversity and create new solutions, while a migration fraction of 0.4 was used to prevent premature convergence and ensure a robust search for optimal results. As a result, the algorithm generates a Pareto-optimal set, which represents a collection of non-dominated solutions, each offering a unique trade-off between the conflicting objectives. These solutions provide insights into the optimal design space and help to select the most suitable combination of input parameters based on desired performance criteria.

To determine the optimum solution among the Pareto-optimal results, the TOPSIS method was used. TOPSIS is a multi-criteria decision-making method that considers multiple criteria with equal weights and selects the solution that offers the best compromise between the output responses [46]. By applying TOPSIS, the optimum combination of input parameters was identified, providing the most desirable balance between effective strain, maximum pressing load, and strain inhomogeneity.

2.5. Experimental Setup

The assembly of the components used in the experiment is shown in Figure 7. The die and die holder were heated to 210 °C by placing 8 resistor rods into the pre-drilled channels of the die holder. The heating process took approximately 90 min. The temperature was maintained at this value using a thermocouple installed in the die holder and a control panel.

Before being placed into the die holder, the die was thoroughly cleaned and lubricated. To minimize friction between the workpiece and the die, a heat-resistant solid lubricant

(Molykote G-n Plus) and a spray lubricant (Sonax MoS₂O) were used. Additionally, the workpieces were preheated in a furnace to the experimental temperature of 210 °C.

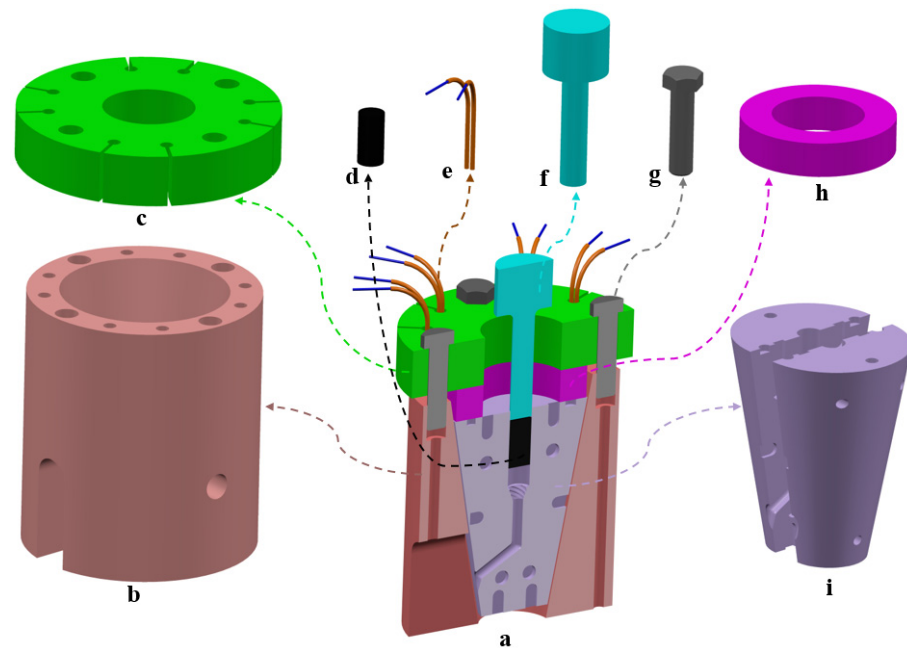


Figure 7. Assembly of parts. (a) Assembly, (b) die holder, (c) fixed part-1, (d) workpiece, (e) resistor rods, (f) punch, (g) M18×20 bolt, (h) fixed part-2, and (i) die.

The pressing speed was set to 1 mm/s. The pressing load applied by the press was continuously monitored and recorded.

Fiber insulation material was placed between the press table and the die holder to minimize heat transfer, helping to maintain a consistent temperature within the die holder during the experiment as shown in Figure 8. Additionally, the die holder was fixed from both sides to prevent any lateral movement, ensuring stability throughout the process. Furthermore, to improve accuracy, the surface was leveled, minimizing any potential displacement of the center during pressing. The digital control panel monitored and maintained the precise processing temperature throughout the experiment. Safety chains were installed around the experimental setup to ensure secure operation. The experiments were conducted using a 150-ton hydraulic press.

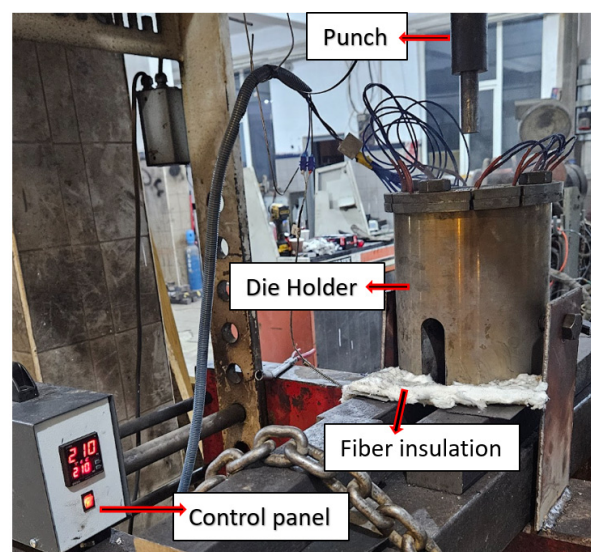


Figure 8. Experimental setup.

2.6. Mechanical Property Investigations

2.6.1. Hardness Tests

To clarify the mechanical properties of specimens, microhardness measurements were also carried out after the Vo-CAP process according to the ASTM E92-Standard Test Method for Vickers. The HVS1000A Vickers hardness tester used with a 500 N load and a 10 s dwell time in a plane perpendicular to the extrusion direction. To obtain accurate measurements, the workpiece was first cut perpendicular to the extrusion direction and then coated with bakallite. Measurements were taken from the coated sample, cut perpendicular to the direction of extrusion, at 1 cm intervals with 10 pieces through the center. Then, the average value was obtained to evaluate and compare the mechanical properties.

2.6.2. Tensile Tests

Tensile tests were conducted with an Instron machine under displacement control according to ASTM standard ASTM, E8 ASTM E8/E8M Standard Test Methods for Tension Testing of Metallic Materials. The test specimens were prepared along the extrusion direction of the Vo-CAP-processed workpieces. The geometry of the test's specimens was specified according to same standard as given in Figure 9a. Test specimens prepared according to ASTM standards are shown in Figure 9b. In order to eliminate undesired errors during experiments, the tests were repeated three times. Then, the average values were taken into consideration.

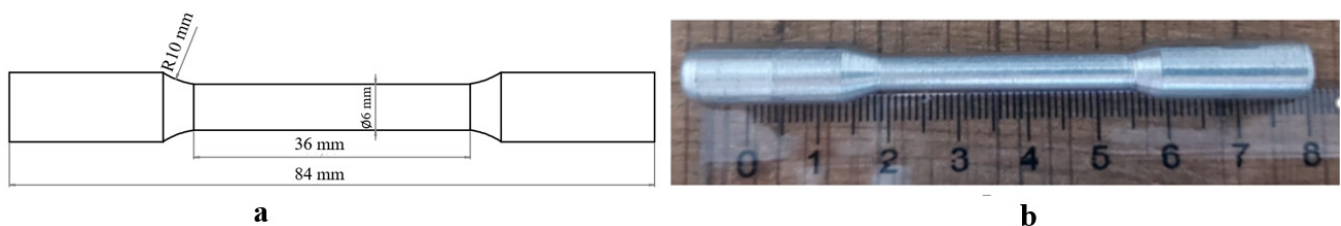


Figure 9. Tensile test sample. (a) Geometrical dimensions. (b) Prepared round test specimen.

2.7. Microstructural Analysis

Optical Microscopy

In order to understand the mechanical properties in detail and to examine the changes in grain levels, microstructural investigations were carried out via obtaining OM images by using a Nikon MA100 optical microscope. In this context, firstly, the workpieces were cut perpendicular along the extrusion directions, the same as in the hardness tests, and then coated with bakallite. Later on, the workpieces were grinded with 320, 800, 1200, 2500, and 4000 grit SiC emery papers, respectively. Furthermore, the workpieces were polished with 1 μ -sized diamond paste. Finally, the workpieces were etched for five seconds with Keller etchant, whose chemical composition is 1% HF, 1.5% HCl, 2.5% HNO₃, and 95% deionized water (DI), and OM images were acquired.

3. Results and Discussion

3.1. Fem Results

Before this extensive work could be undertaken, it was necessary to validate the FEM setup and assess whether the novel Vo-CAP die design would give better results compared to VE. To achieve this, the FEM model was validated against the study conducted by Shahbaz et al. using identical material properties, boundary conditions, and process parameters for the AA1050 workpiece [24]. As shown in Figure 10, there is excellent agreement between the simulation results obtained in this study and the reference data at different twist angles (30°, 90°, and 180°). This clearly confirms the reliability of the FEM

setup designed for this study. Furthermore, as is clearly evident in the figure, the Vo-CAP method consistently achieves both higher strain values and more homogeneous effective strain distributions compared to VE.

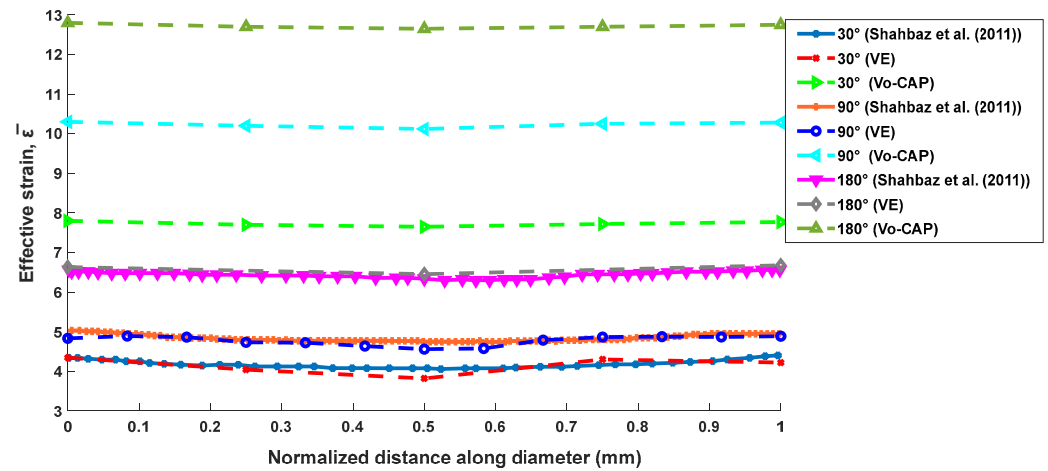


Figure 10. Validation of the FEM setup and comparison of the VE and the Vo-CAP at different twist angles [24].

To systematically investigate the effects of geometric parameters on the Vo-CAP process performance, twenty-seven different die configurations were analyzed using FEM. Table 3 presents the comprehensive results of these analyses, showing the relationship between design variables (β , T_L , and TC_L) and objectives ($\bar{\epsilon}$, ML , and $CV_{\epsilon p}$).

Table 3. FEM results for 27 die designs.

Case Num.	Variables			Objectives		
	β	T_L	TC_L	$\bar{\epsilon}$	ML	$CV_{\epsilon p}$
case 1	30	10	10	11.84	12.79	0.434
case 2	30	10	25	11.66	13.29	0.440
case 3	30	10	50	9.32	13.87	0.350
case 4	30	20	10	11.32	13.63	0.429
case 5	30	20	25	9.41	13.7	0.414
case 6	30	20	50	6.23	13.88	0.330
case 7	30	40	10	7.81	14.96	0.407
case 8	30	40	25	7.22	15.05	0.416
case 9	30	40	50	7.12	15.27	0.330
case 10	90	10	10	13.15	13.73	0.401
case 11	90	10	25	12.13	14.23	0.392
case 12	90	10	50	9.87	14.44	0.349
case 13	90	20	10	12.04	13.87	0.428
case 14	90	20	25	10.16	13.92	0.404
case 15	90	20	50	8.17	14.66	0.340
case 16	90	40	10	7.31	15.12	0.426
case 17	90	40	25	7.28	15.17	0.417
case 18	90	40	50	7.25	15.2	0.339
case 19	180	10	10	20.04	16.05	0.463
case 20	180	10	25	17.36	16.87	0.489
case 21	180	10	50	13.96	16.91	0.385
case 22	180	20	10	15.03	15.99	0.462
case 23	180	20	25	13.89	16.13	0.446
case 24	180	20	50	13.01	16.4	0.392
case 25	180	40	10	8.52	16.33	0.454
case 26	180	40	25	7.81	16.48	0.458
case 27	180	40	50	7.52	16.83	0.384

The results demonstrate that the twist angle (β) has a significant impact on effective strain values. Higher twist angles tend to increase the effective strain but also result in greater maximum pressing loads. Furthermore, increasing the channel length (C_L)

improves strain homogeneity; however, it negatively affects the effective strain. These opposing effects of the design variables on the different objectives highlight the complexity of the optimization problem. Therefore, a comprehensive multi-objective optimization approach was necessary to identify the optimal design parameters that balance these competing factors.

To better understand the process mechanics, Figure 11 shows both the deformation patterns and the load–stroke curve during the Vo-CAP process. The process can be divided into three zones. Each zone shows a specific characteristic behavior. In the VE zone, a rapid pressing load increase was observed from 0 to 5.6 mm of the stroke. This is due to the fact that the material has been forced into the vortex-shaped channel. And the result is torsional deformation, which necessitates considerable pressing load. In the TC zone, the pressing load was relatively constant from about 5.8 mm to 15.1 mm of the die stroke. So, this zone has, therefore, acted as a bridge between the VE and ECAP regions. As the material flows through a straight channel without much deformation, the force was stable in this TC zone. In the final ECAP zone, at approximately 15 mm of the die stroke, the pressing load was suddenly increased. As the material entered the third and final ECAP section, it was subjected to high shear deformation due to the sharp rotation. As the fluidity of the material increases at this point and the resistance exerted by the die decreases, the pressing load was reduced slightly between the 35 and 40 mm range of the stroke.

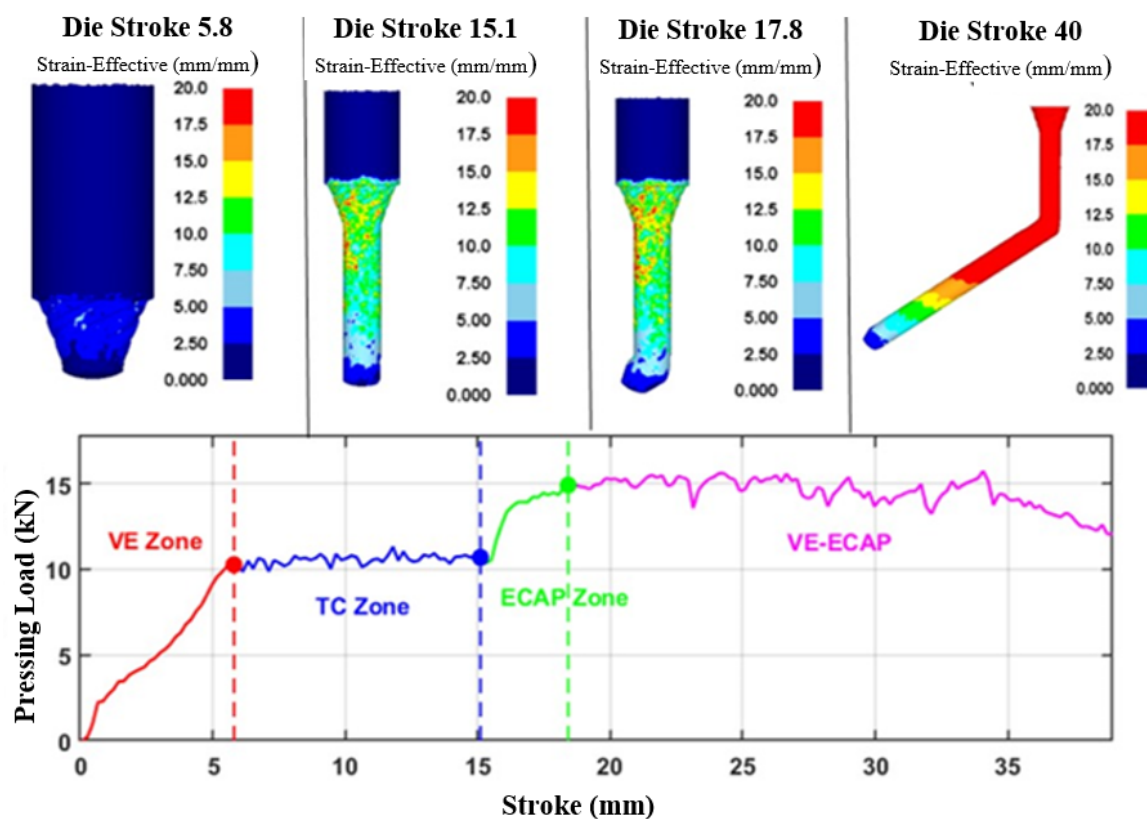


Figure 11. Zones of Vo-CAP process and stroke–pressing load curve.

To ensure that the material achieved the desired vortex shape, the experiment was paused, and the die was opened to inspect the deformation progress. This step-by-step inspection confirmed that the material was following the expected forming pattern, further supporting the reliability of the FEM model in predicting the material's behavior under these conditions.

The comparison between experimental results and FEM predictions shows a close alignment in both shape and pressing load throughout the forming process, as illustrated

in Figure 12. Each stage demonstrates strong agreement between the FEM model and experimental measurements. In particular, the fact that the material discharge cross-sectional images, as shown with red dashed lines in Figure 12, in the experimental results are almost identical to those obtained as a result of FEM simulations proves the accuracy of the model in capturing the final shape.

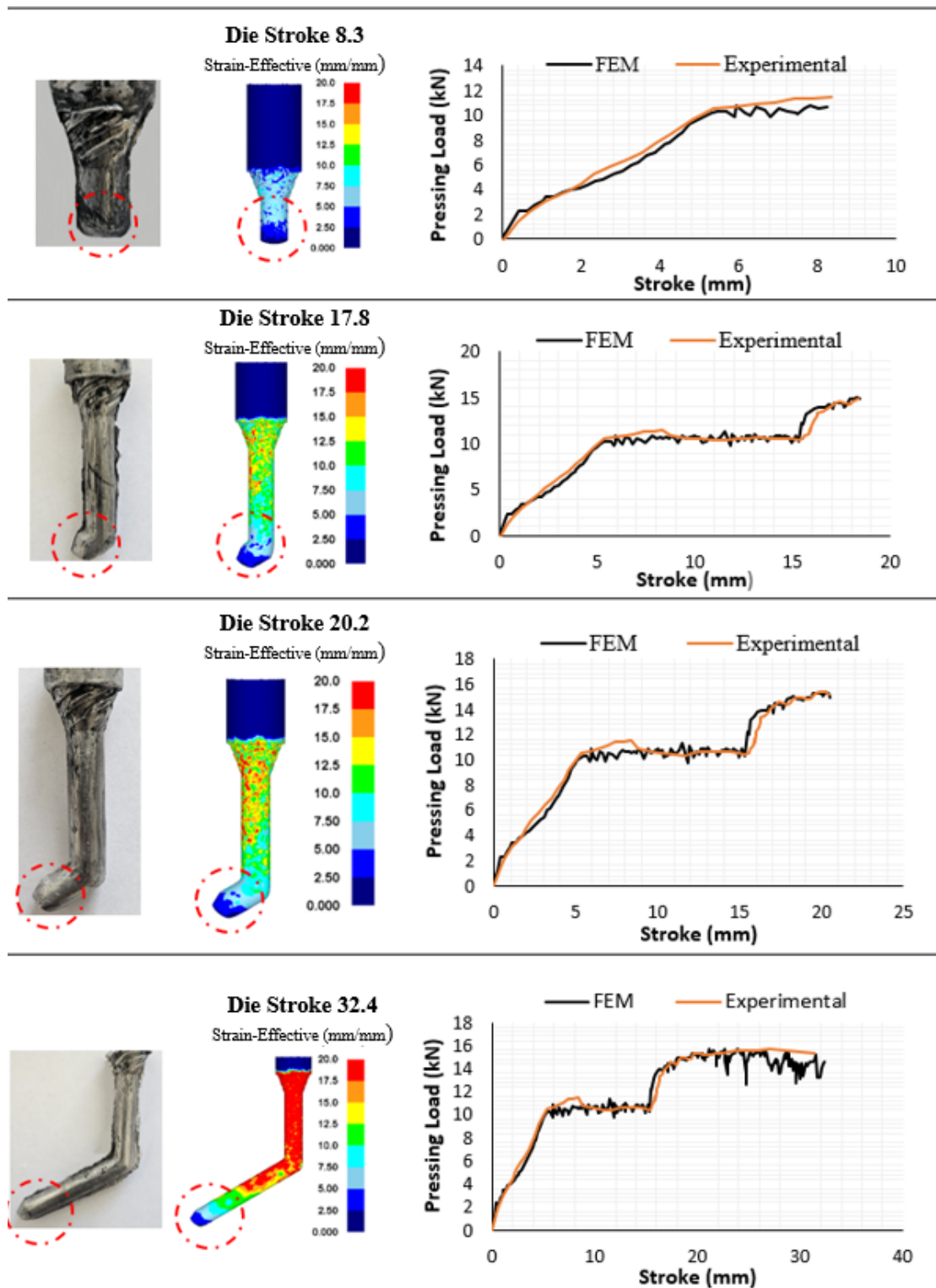


Figure 12. Comparison of experimental and FEM results during different stages of Vo-CAP process: experimental samples (left), effective strain distributions (middle), and pressing load–stroke curves (right) at die strokes of 8.3, 17.8, 20.2, and 32.4 mm.

3.2. Optimization Results

The trained ANN model demonstrated excellent prediction capability for output responses, as shown in Figure 13. The model achieved high accuracy with R-squared values of 0.992, 0.988, and 0.971 for effective strain, maximum pressing load, and strain inhomogeneity, respectively. The corresponding low MSE values of 0.090, 0.018, and 0.010 further confirm the model's reliability. As seen in Figure 13a–c, the comparison between predicted and actual values shows a strong correlation, indicating that the ANN successfully captured the nonlinear relationships between input parameters and output responses. This high predictive accuracy validates the ANN model's capability to effectively map the complex relationships in the Vo-CAP process.

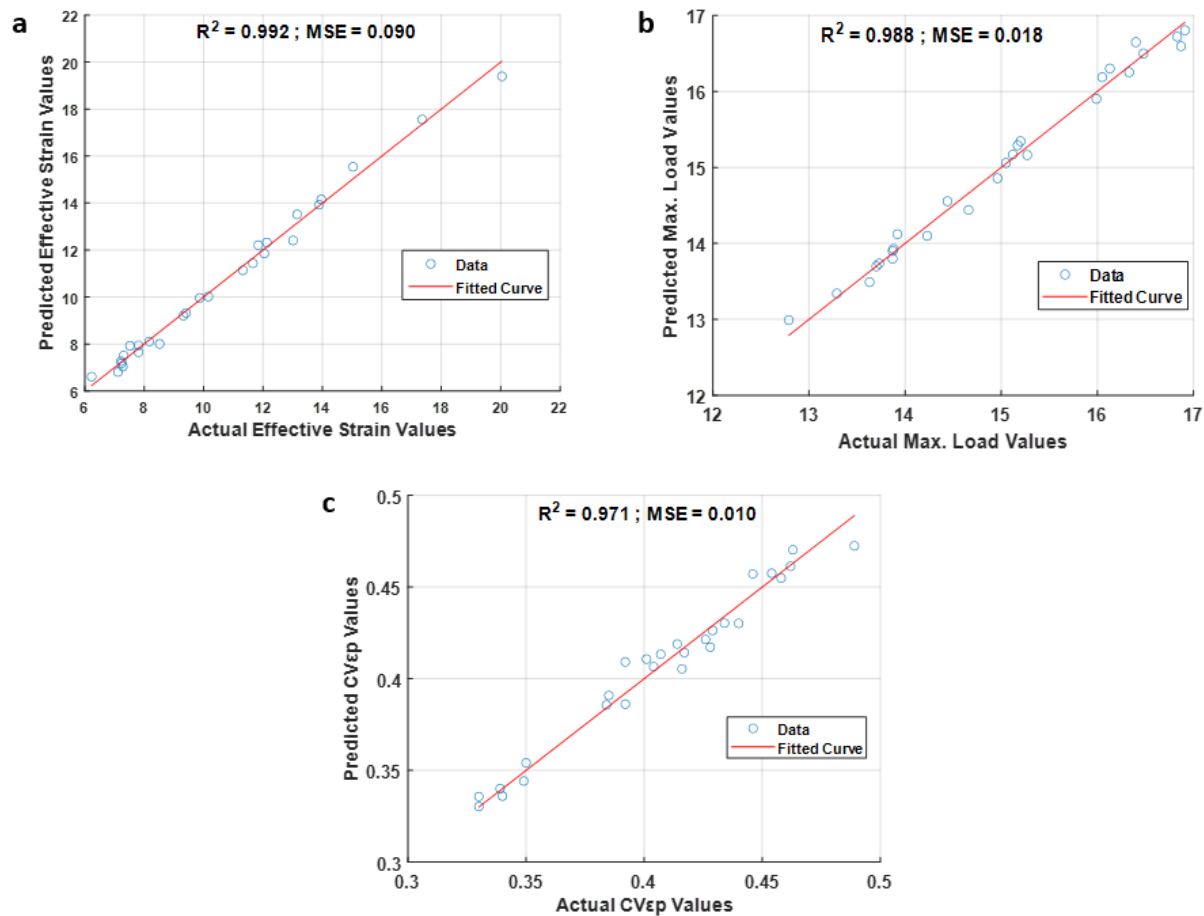


Figure 13. The comparison between prediction values and targets of (a) effective strain, (b) max. pressing load, and (c) strain inhomogeneity.

Later on, by using the best-performing networks obtained through the trained ANN model, the NSGA-II optimization process resulted in 35 Pareto-optimal solutions as shown in Figure 14. Subsequently, the TOPSIS method was applied, assigning equal weights to each objective, to identify the most balanced solution among these Pareto-optimal results. As shown in the figure, the identified optimal solution corresponds to an effective strain of 16.49, a maximum pressing load of 15.69 kN, and a coefficient of strain inhomogeneity of 0.375. This optimal point, highlighted in red in the figure, represents the best compromise between maximizing effective strain while simultaneously minimizing both the strain inhomogeneity and maximum pressing load.

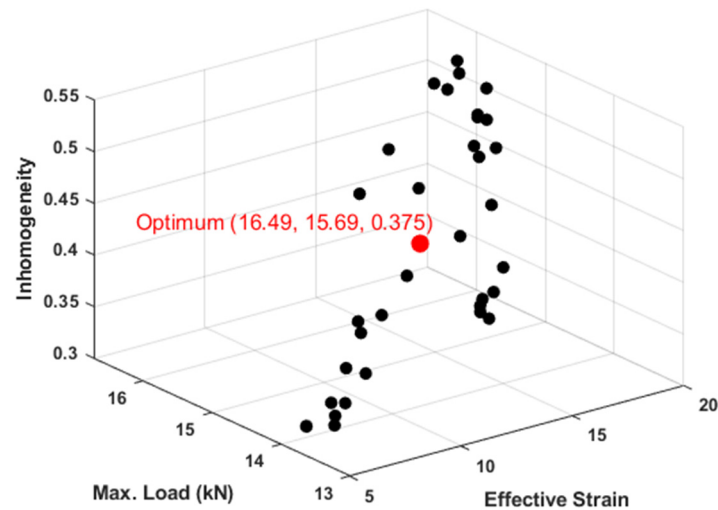


Figure 14. Pareto-optimal solutions generated by NSGA-II (optimum point $\bar{\epsilon} = 16.49$, $ML = 15.69$, and $CV\epsilon_p = 0.375$).

The optimal design parameters were determined at a twist angle of 166.33° , T_L of 10.33 mm, and TC_L of 34.2 mm. To validate the optimization results, a new FEM analysis was performed using these optimal parameters. The simulation results showed excellent agreement with the predicted optimization values: a maximum pressing load of 15.65 kN (compared to the predicted 15.69 kN) as seen in Figure 11, an effective strain of 16.60 (compared to the predicted 16.49), and a strain inhomogeneity of 0.378 (compared to the predicted 0.375). This close correlation between optimization predictions and FEM results validates the accuracy of our optimization approach. The reason for the T_L value being close to the lower bound is that, as shown in Table 3, increasing the T_L value leads to a decrease in effective strain values while simultaneously increasing the pressing load. Strain inhomogeneity is only partially affected by changes in the T_L value. Following this successful validation, the optimized die was manufactured, with its geometrical details shown in Figure 15.

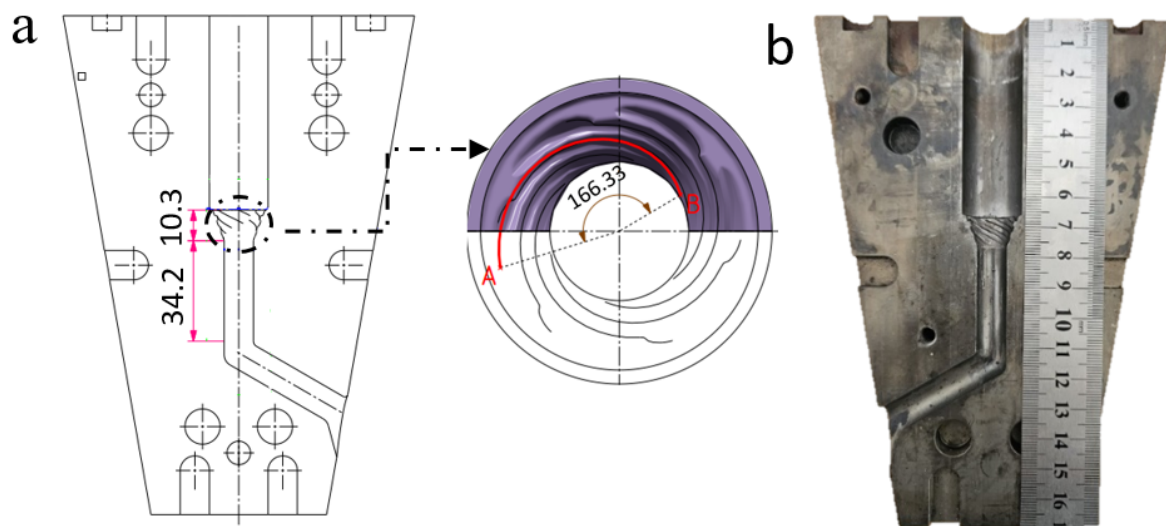


Figure 15. Optimum design variables of Vo-CAP. (a) Geometrical details. (b) Manufactured Vo-CAP die.

3.3. Experimental Results

The experimental studies for the Vo-CAP process were carried out on the manufactured die in accordance with the optimized process parameters. During the process, the workpiece emerges from the channel marked with red dashed lines as shown in Figure 16a. The die's conical design allows for easy assembly and disassembly without using tradi-

tional fasteners like bolts or nuts. The resistor rods and thermocouples integrated into the die holder kept the processing temperature constant at 210 °C throughout the experiments.



Figure 16. (a) View of the workpiece (red dashed line) emerging through the exit channel during the Vo-CAP process. (b) Vo-CAP-processed AA6082.

The processed AA6082 workpieces, as shown in Figure 16b, demonstrate the successful implementation of the Vo-CAP process. The workpiece show uniform deformation along its length, with no visible surface defects or irregularities, indicating stable material flow during processing. The dimensional consistency of the processed workpiece confirms the precision of the manufacturing process and the effectiveness of the die design.

The unprocessed workpiece shown in Figure 17 clearly demonstrates the effectiveness of the Vo-CAP process. The workpiece has taken the precise shape of the die channel geometry, showing both the VE and ECAP channel. This processed part demonstrates that the workpiece successfully flowed through all stages of the die, maintaining the designed forming patterns. The shape particularly highlights the combined effect of both the vortex and ECAP deformation mechanisms.



Figure 17. Deformation path geometry in Vo-CAP die.

3.4. Mechanical Property Investigation Results

3.4.1. Hardness Test Results

Due to hardness tests' simplicity and the fact that hardness is an important criterion in material selection, it is one of the mechanical properties which are primarily investigated in material enhancement studies such as SPD studies. Given these characteristics, this study was primarily aimed at investigating how the hardness of the material changed. In this context, hardness tests were performed according to standards, and the results are given in Figure 18. When the obtained results were examined, it can be seen that the hardness values for annealed AA6082 were acquired at about 50 HV. Similar results for annealed AA6082 workpieces at 53 HV have been reported in other studies [35,58–60] and can be easily found in the literature. This close result is a confirmation of the hardness values obtained in this study. Again, when other studies in the literature were examined, the hardness value for AA6082 processed with multipass ECAP was found to be 115 HV, which is an increase over the annealed material [59–61]. However, after the one-pass Vo-CAP process, this enhancement is reached and the average hardness value of 113.2 HV was obtained after only one pass, which is approximately double when compared to the annealed material. Furthermore, when examining the figure, it can be seen that more hardness is gained when moving away from the center. The reason for this is that the frictional resistance, which prevents the material from flowing under the applied pressing load, is greater at the edges. Accordingly, the stress value applied per particle is higher. When the values of the hardness results obtained are analyzed, it is seen that the distribution correlates with the effective strain results.

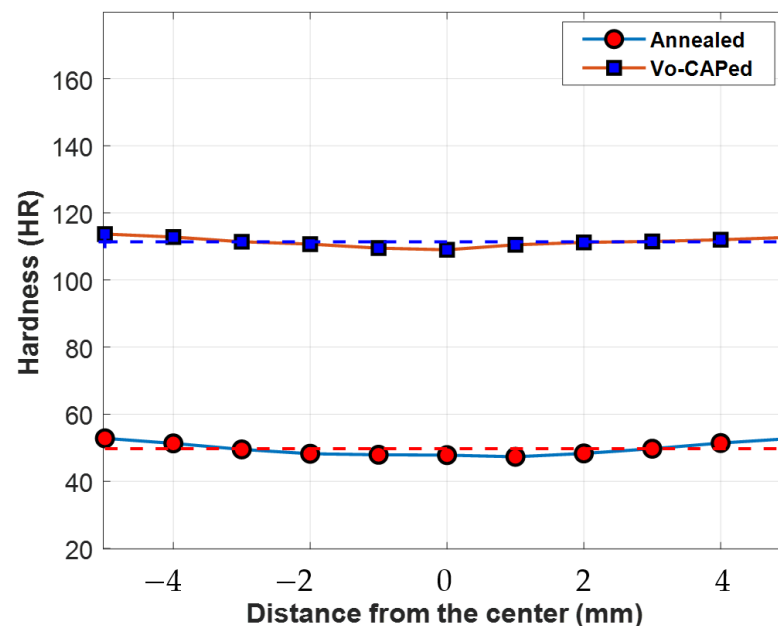


Figure 18. Hardness values of annealed and Vo-CAP-processed samples.

3.4.2. Tensile Test Results

To be able to observe the mechanical property enhancements of the workpieces after Vo-CAP processes, a tensile test was conducted, and the obtained stress–strain diagram is illustrated in Figure 19. As mentioned before, the comparison was carried out between annealed and multipass ECAP-processed workpieces. According to the literature, the ultimate tensile strength (UTS) value for annealed AA6082 workpieces is about 135 MPa and was obtained by [59,62]. In this study, the UTS value was 143,94 MPa, which is very similar to the reference studies. After the multipass ECAP process, a UTS value of about 350 MPa was obtained, which is much better than annealed workpieces [59]. In return for

this novel study, after the Vo-CAP process, the obtained UTS value was 420 MPa, which is better than both the annealed and multipass-processed workpieces. So, it is easy to say that the mechanical property of AA6082 workpieces was enhanced after the Vo-CAP process.

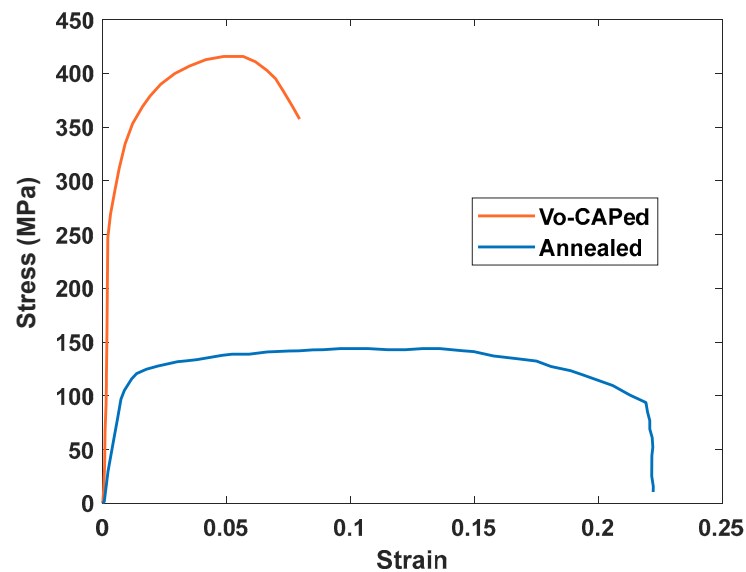


Figure 19. Stress–strain curve of annealed and Vo-CAP-processed samples.

Moreover, the fracture surface of the tensile test specimen exhibits a 45-degree shear failure mode, as indicated by the red dashed line in Figure 20.

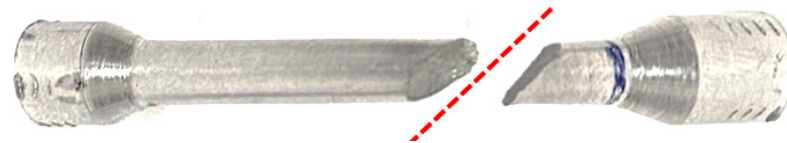


Figure 20. Fracture surface of tensile test specimen.

A similar enhancement was acquired after the Vo-CAP process in terms of both the yield strength and toughness values. The obtained results are given in Table 4. The yield strength value increased from 92 MPa to 248 MPa after the Vo-CAP process compared to annealed material. The result is a further improvement in the material's elasticity properties. This conclusion can also be reached clearly when the elongation-at-break values are analyzed. While this value was 22.43% for annealed material, this value was reduced to 8.12% as a result of the Vo-CAP process as illustrated in Table 4.

Table 4. Comparison of mechanical properties of annealed and Vo-CAP-processed AA6082.

Sample	YS (MPa)	UTS (MPa)	Elongation at Break (%)	Hardness (HV)	Toughness MJ/m ³
Annealed AA6082	92	143.94	22.43	49.5	27.74
Vo-CAP AA6082	248	415.75	8.12	113.2	30.09

When the obtained results were compared in terms of toughness, after the Vo-CAP process, the calculated value was 30.09 MJ/m³ [Table 4]. When the literature is examined, the toughness was generally reduced after the one-pass ECAP process. This is due to a reduction in the elongation of the material as a result of an insufficient number of passes through the ECAP process [63]. In comparison with the annealed material, although the toughness value decreases after the single-pass ECAP process, this value does not decrease and increases slightly as a result of this novel Vo-CAP process, indicating that the process also gives more efficient results for this parameter.

3.5. Microstructural Characterization Results

The main focus of this study is to increase the efficiency of the Vo-CAP process, which is presented to the literature as a novel SPD method, through optimization studies. Furthermore, another main objective is to make the process more applicable by eliminating the fasteners that cause major time losses and process difficulties during SPD processes, thanks to the conical geometry used for the design of the Vo-CAP die, and to pioneer its use within the industry. Therefore, microstructure investigations were limited to OM analysis only.

Optical Microscopy Characterization

OM images were taken to gain a better understanding of the mechanical tests that were carried out to see the effects of this Vo-CAP process on the material properties and to observe the possible particle orientations. In Figure 21, the obtained OM images are illustrated for annealed and Vo-CAP-processed workpieces. In Figure 21a, a 500x-zoomed OM image is given for annealed AA6082. When the image is examined, it can be said the secondary phases were distributed homogeneously thanks to the annealing process. But the grain boundaries could not be specified by only OM images. But, after the Vo-CAP process was conducted again, the grain boundaries could not be observed. This meant that the expected grain size reductions resulting from Vo-CAP processing could not be studied using OM images. However, it is clear that the grains were oriented as shown in Figure 21b. This is one of the key factors explaining the enhancement of mechanical properties after the Vo-CAP process. The primary focus of this study is on die design, optimization, and experimental feasibility and applicability, as opposed to the effect of the process on the grains. It is evident that, owing to the unavailability of detailed information from the OM images obtained, the observation of particle shrinkage and orientation was deemed sufficient to demonstrate the effect of the process on the material's particles. Consequently, OM images were employed, and no additional detailed microstructural analysis was deemed necessary in this study.

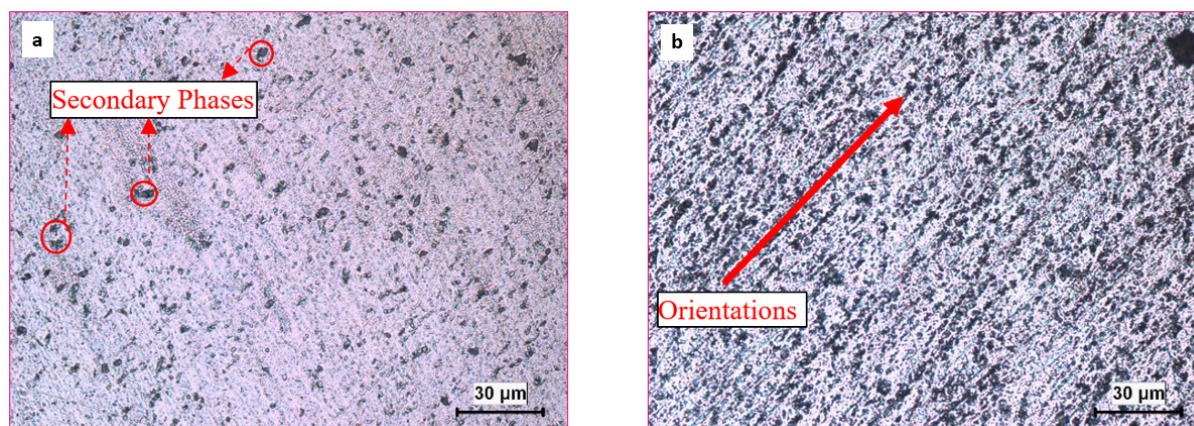


Figure 21. OM images. (a) Annealed and (b) Vo-CAP-processed workpiece.

4. Conclusions

This study introduced a novel hybrid SPD technique called Vo-CAP, which combines the advantages of both VE and ECAP processes in a single die. The innovative design features a unique integration of Vortex Extrusion and ECAP channels, complemented by a conical die geometry that enables efficient assembly and disassembly without traditional fasteners. This single-pass process configuration enhances its suitability for industrial implementation.

The research methodology encompassed a comprehensive FEA, ANN, and NSGA-II algorithm and experimental studies. The process parameters were systematically optimized using a multi-objective approach that considered effective strain, pressing load, and strain inhomogeneity. The optimal design parameters were determined to be a twist angle of 166.33° , twist length of 10.33 mm, and Transition Channel length of 34.2 mm. The optimization results were validated through both FEM analysis and experimental studies, showing excellent agreement.

The experimental results demonstrated significant improvements in mechanical properties of AA6082 aluminum alloy:

- Hardness increased to 113.2 HV, representing a twofold improvement compared to the annealed state;
- Ultimate tensile strength reached 415.75 MPa, and yield strength increased to 248 MPa;
- Material toughness was improved compared to the annealed state, demonstrating an enhanced energy absorption capability;
- OM images clearly show the homogeneous distribution of the annealed material. In addition, orientations were clearly seen in the OM images obtained as a result of the Vo-CAP process. Since the OM images were adequate to see a grain size reduction and grain orientations, another detailed microstructural analysis was not required in this study;
- The strain distribution showed improved homogeneity across the processed workpieces;
- The single-pass processing capability reduced processing time and energy consumption;
- The assembly and operation were simplified through the innovative conical die design.

These results demonstrate that the Vo-CAP process represents a significant advancement in SPD techniques, showing effectiveness in enhancing the mechanical properties of AA6082 aluminum alloy through grain refinement.

SPD methods generally result in very good mechanical properties, but what makes them more attractive than the conventional method is that the ductility of the material does not decrease after the process. Nevertheless, the fact that SPD processes are only suitable for small-scale materials appears to be the most significant challenge to their industrial application. Looking at the industrial uses of small aluminum alloys, they are used as fasteners such as nuts, bolts, and rivets, particularly in the aerospace industry. Considering, for example, that the operating conditions of an aircraft are -60 degrees at an altitude of 10,000 feet and $+30$ degrees on the ground, it is certain that increasing the mechanical life of these simple and cheap-looking fasteners will be an important gain in terms of reducing the time the aircraft spends in the hangar, if not in terms of fastener costs. For this reason, such methods are believed to have a great deal of potential for industrial applications.

The alloy of choice for this study was AA6082, which is often the preferred alloy for SPD processes. And the Vo-CAP process was successfully completed. The literature shows that SPD studies have been successfully applied to various metallic parts including other aluminum alloys, copper, magnesium, steel, etc. Therefore, it will not be difficult to say that this method, which is presented in the literature as a new SPD method and offers ease of use and time saving, can be applied to other materials used in SPD studies. Consequently, while the current study focuses specifically on AA6082, future research could explore the potential applicability of this process to other metallic materials.

As a result, the successful implementation and validation of this novel technique opens new possibilities for materials processing and property enhancement in industrial applications.

Author Contributions: Conceptualization, H.B. and K.Ö.; supervision, Ş.T.; methodology, H.B. and K.Ö., investigation, H.B., K.Ö. and Ş.T.; software, H.B. and K.Ö.; writing—review and editing, H.B., K.Ö. and Ş.T. All authors have read and agreed to the published version of the manuscript.

Funding: This work was supported by the Scientific Research Projects Unit (BAPSIS) of Inonu University through the project number ‘FDK-2022-2999’.

Institutional Review Board Statement: Not applicable.

Informed Consent Statement: Not applicable.

Data Availability Statement: The data presented in this study are available on request from the corresponding author due to ongoing research.

Conflicts of Interest: The authors declare no conflicts of interest.

References

- Huang, Y.; Langdon, T.G. Advances in ultrafine-grained materials. *Mater. Today* **2013**, *16*, 85–93. [\[CrossRef\]](#)
- Valiev, R.Z.; Islamgaliev, R.K.; Alexandrov, I.V. Bulk nanostructured materials from severe plastic deformation. *Prog. Mater. Sci.* **2000**, *45*, 103–189. [\[CrossRef\]](#)
- Hall, E. The deformation and ageing of mild steel: III discussion of results. *Proc. Phys. Society. Sect. B* **1951**, *64*, 747. [\[CrossRef\]](#)
- Petch, N.J. The cleavage strength of polycrystals. *J. Iron Steel Inst.* **1953**, *174*, 25–28.
- Segal, V. Plastic working of metals by simple shear. *Russ. Metall. (Engl. Transl.)* **1981**, *1*, 99.
- Valiev, R.Z.; Langdon, T.G. Principles of equal-channel angular pressing as a processing tool for grain refinement. *Prog. Mater. Sci.* **2006**, *51*, 881–981. [\[CrossRef\]](#)
- Purcek, G.; Saray, O.; Kul, O.; Karaman, I.; Yapici, G.; Haouaoui, M.; Maier, H. Mechanical and wear properties of ultrafine-grained pure Ti produced by multi-pass equal-channel angular extrusion. *Mater. Sci. Eng. A* **2009**, *517*, 97–104. [\[CrossRef\]](#)
- Şahbaz, M.; Kaya, H.; Kentli, A.; Uçar, M.; Ögüt, S.; Özbeyaz, K. Analytical and numerical analysis comparison of equal channel angular pressing for Al5083 alloy. *Adv. Sci. Eng. Med.* **2019**, *11*, 1100–1103. [\[CrossRef\]](#)
- Kaya, H.; Özbeyaz, K.; Kentli, A. Mechanical property improvement of a AA6082 alloy by the TV-CAP process as a novel SPD method. *Mater. Test.* **2023**, *65*, 244–257. [\[CrossRef\]](#)
- Özbeyaz, K.; Kaya, H.; Kentli, A. Novel SPD method: Twisted variable channel angular extrusion. *Met. Mater. Int.* **2022**, *28*, 1290–1305. [\[CrossRef\]](#)
- Valiev, R.; Kuznetsov, O.; Musalimov, R.S.; Tsenev, N. Low-temperature superplasticity of metallic materials. *Dokl. Akad. Nauk. SSSR.* **1988**, *301*, 864–866.
- Zhilyaev, A.P.; Langdon, T.G. Using high-pressure torsion for metal processing: Fundamentals and applications. *Prog. Mater. Sci.* **2008**, *53*, 893–979. [\[CrossRef\]](#)
- Saito, Y.; Utsunomiya, H.; Tsuji, N.; Sakai, T. Novel ultra-high straining process for bulk materials—Development of the accumulative roll-bonding (ARB) process. *Acta Mater.* **1999**, *47*, 579–583. [\[CrossRef\]](#)
- Tsuji, N.; Saito, Y.; Lee, S.H.; Minamino, Y. ARB (Accumulative Roll-Bonding) and other new techniques to produce bulk ultrafine grained materials. *Adv. Eng. Mater.* **2003**, *5*, 338–344. [\[CrossRef\]](#)
- Derakhshan, J.F.; Parsa, M.; Jafarian, H. Microstructure and mechanical properties variations of pure aluminum subjected to one pass of ECAP-Conform process. *Mater. Sci. Eng. A* **2019**, *747*, 120–129. [\[CrossRef\]](#)
- Ghaforian Nosrati, H.; Khalili, K.; Gerdooei, M. Theoretical and numerical investigation of required torque in ECAP-Conform process. *Metall. Mater. Trans. B* **2020**, *51*, 519–528. [\[CrossRef\]](#)
- Xu, C.; Schroeder, S.; Berbon, P.B.; Langdon, T.G. Principles of ECAP-Conform as a continuous process for achieving grain refinement: Application to an aluminum alloy. *Acta Mater.* **2010**, *58*, 1379–1386. [\[CrossRef\]](#)
- Mckenzie, P.W.J.; Lapovok, R.; Estrin, Y. The influence of back pressure on ECAP processed AA 6016: Modeling and experiment. *Acta Mater.* **2007**, *55*, 2985–2993. [\[CrossRef\]](#)
- Stolyarov, V.; Lapovok, R. Effect of backpressure on structure and properties of AA5083 alloy processed by ECAP. *J. Alloys Compd.* **2004**, *378*, 233–236. [\[CrossRef\]](#)
- Nishida, Y.; Arima, H.; Kim, J.-C.; Ando, T. Rotary-die equal-channel angular pressing of an Al–7 mass% Si–0.35 mass% Mg alloy. *Scr. Mater.* **2001**, *45*, 261–266. [\[CrossRef\]](#)
- Qarni, M.J.; Sivaswamy, G.; Rosochowski, A.; Boczkal, S. Effect of incremental equal channel angular pressing (I-ECAP) on the microstructural characteristics and mechanical behaviour of commercially pure titanium. *Mater. Des.* **2017**, *122*, 385–402. [\[CrossRef\]](#)
- Ögüt, S.; Kaya, H.; Kentli, A.; Uçar, M. Applying hybrid equal channel angular pressing (HECAP) to pure copper using optimized Exp.-ECAP die. *Int. J. Adv. Manuf. Technol.* **2021**, *116*, 3859–3876. [\[CrossRef\]](#)
- Shahbaz, M.; Ebrahimi, R.; Kim, H. Streamline approach to die design and investigation of material flow during the vortex extrusion process. *Appl. Math. Model.* **2016**, *40*, 3550–3560. [\[CrossRef\]](#)

24. Shahbaz, M.; Pardis, N.; Ebrahimi, R.; Talebanpour, B. A novel single pass severe plastic deformation technique: Vortex extrusion. *Mater. Sci. Eng. A* **2011**, *530*, 469–472. [\[CrossRef\]](#)
25. Shahbaz, M.; Pardis, N.; Kim, J.; Ebrahimi, R.; Kim, H. Experimental and finite element analyses of plastic deformation behavior in vortex extrusion. *Mater. Sci. Eng. A* **2016**, *674*, 472–479. [\[CrossRef\]](#)
26. Ranjbari, G.; Doniavi, A.; Shahbaz, M. Numerical modelling and simulation of vortex extrusion as a severe plastic deformation technique using response surface methodology and finite element analysis. *Met. Mater. Int.* **2021**, *27*, 2898–2909. [\[CrossRef\]](#)
27. Pardis, N.; Ebrahimi, R. Deformation behavior in Simple Shear Extrusion (SSE) as a new severe plastic deformation technique. *Mater. Sci. Eng. A* **2009**, *527*, 355–360. [\[CrossRef\]](#)
28. Pardis, N.; Ebrahimi, R. Different processing routes for deformation via simple shear extrusion (SSE). *Mater. Sci. Eng. A* **2010**, *527*, 6153–6156. [\[CrossRef\]](#)
29. Ebrahimi, M.; Djavanroodi, F. Experimental and numerical analyses of pure copper during ECFE process as a novel severe plastic deformation method. *Prog. Nat. Sci. Mater. Int.* **2014**, *24*, 68–74. [\[CrossRef\]](#)
30. Ebrahimi, M.; Tiji, S.N.; Djavanroodi, F. Upper bound solution of equal channel forward extrusion process as a new severe plastic deformation method. *Metall. Res. Technol.* **2015**, *112*, 609. [\[CrossRef\]](#)
31. Chen, Q.; Zhao, Z.; Zhao, Z.; Hu, C.; Shu, D. Microstructure development and thixoextrusion of magnesium alloy prepared by repetitive upsetting-extrusion. *J. Alloys Compd.* **2011**, *509*, 7303–7315. [\[CrossRef\]](#)
32. Lianxi, H.; Yuping, L.; Erde, W.; Yang, Y. Ultrafine grained structure and mechanical properties of a LY12 Al alloy prepared by repetitive upsetting-extrusion. *Mater. Sci. Eng. A* **2006**, *422*, 327–332. [\[CrossRef\]](#)
33. Landgrebe, D.; Sterzing, A.; Schubert, N.; Bergmann, M. Influence of die geometry on performance in gradation extrusion using numerical simulation and analytical calculation. *CIRP Ann.* **2016**, *65*, 269–272. [\[CrossRef\]](#)
34. Neugebauer, R.; Sterzing, A.; Selbmann, R.; Zachäus, R.; Bergmann, M. Gradation extrusion–Severe plastic deformation with defined gradient. *Mater. Werkst.* **2012**, *43*, 582–588. [\[CrossRef\]](#)
35. Kaya, H.; Uçar, M.; Şahbaz, M.; Kentli, A.; Özbeyaz, K.; Ögüt, S. Microstructure development and mechanical behaviour of pure copper processed by the novel TWO-CAP procedure. *Mater. Test.* **2023**, *65*, 1209–1221. [\[CrossRef\]](#)
36. Şahbaz, M.; Kaya, H.; Kentli, A. A new severe plastic deformation method: Thin-walled open channel angular pressing (TWO-CAP). *Int. J. Adv. Manuf. Technol.* **2020**, *106*, 1487–1496. [\[CrossRef\]](#)
37. Şahbaz, M.; Kentli, A.; Kaya, H. Performance of novel TWO-CAP (thin-walled open channel angular pressing) method on AA5083. *Met. Mater. Int.* **2021**, *27*, 2430–2437. [\[CrossRef\]](#)
38. Bisadi, H.; Mohamadi, M.R.; Miyanaji, H.; Abdoli, M. A modification on ECAP process by incorporating twist channel. *J. Mater. Eng. Perform.* **2013**, *22*, 875–881. [\[CrossRef\]](#)
39. Mani, B.; Paydar, M. Application of forward extrusion-equal channel angular pressing (FE-ECAP) in fabrication of aluminum metal matrix composites. *J. Alloys Compd.* **2010**, *492*, 116–121. [\[CrossRef\]](#)
40. Paydar, M.; Reihanian, M.; Bagherpour, E.; Sharifzadeh, M.; Zarinejad, M.; Dean, T. Consolidation of Al particles through forward extrusion-equal channel angular pressing (FE-ECAP). *Mater. Lett.* **2008**, *62*, 3266–3268. [\[CrossRef\]](#)
41. Khelfa, T.; Muñoz-Bolaños, J.A.; Li, F.; Cabrera-Marrero, J.M.; Khitouni, M. Microstructure and mechanical properties of AA6082-T6 by ECAP under warm processing. *Met. Mater. Int.* **2020**, *26*, 1247–1261. [\[CrossRef\]](#)
42. Baig, M.; El-Danaf, E.; Mohammed, J.A. A Study on the Synergistic Effect of ECAP and Aging Treatment on the Mechanical Properties of AA6082. *J. Mater. Eng. Perform.* **2016**, *25*, 5252–5261. [\[CrossRef\]](#)
43. Balasubramanian, M.; Sadasivan, N.; Murali, S. Influence of processing route on bonding of AA6082 and MgAZ31B by severe plastic deformation process. *Mater. Today Proc.* **2021**, *46*, 3716–3722. [\[CrossRef\]](#)
44. Agarwal, K.M.; Singh, P.; Dixit, S.; Sergeevna, M.T.; Soloveva, O.; Solovev, S.; Kumar, K. Optimization of die design parameters in ECAP for sustainable manufacturing using response surface methodology. *Int. J. Interact. Des. Manuf. (IJIDeM)* **2024**, *18*, 2903–2910. [\[CrossRef\]](#)
45. Xu, S.; Zhao, G.; Ma, X.; Ren, G. Finite element analysis and optimization of equal channel angular pressing for producing ultra-fine grained materials. *J. Mater. Process. Technol.* **2007**, *184*, 209–216. [\[CrossRef\]](#)
46. Wang, C.; Yoon, K. Multiple attribute decision making. *Lect. Notes Econ. Math. Syst.* **1981**, *404*, 287–288.
47. Karabey, Ö. Design, Finite Element Analysis and Optimization of Helical Angular Pressing (HAP) Method as a Novel SPD Technique. *Bitlis Eren Üniversitesi Fen Bilim. Derg.* **2023**, *12*, 959–968. [\[CrossRef\]](#)
48. Tkocz, M.; Kowalczyk, K.; Bulzak, T.; Jabłońska, M.B.; Hawryluk, M. Finite element analysis of material deformation behaviour during DRECE: The sheet metal SPD process. *Arch. Civ. Mech. Eng.* **2023**, *23*, 145. [\[CrossRef\]](#)
49. Zhang, D.; Hu, H.; Pan, F.; Yang, M.; Zhang, J. Numerical and physical simulation of new SPD method combining extrusion and equal channel angular pressing for AZ31 magnesium alloy. *Trans. Nonferrous Met. Soc. China* **2010**, *20*, 478–483. [\[CrossRef\]](#)
50. Ögüt, S.; Kaya, H.; Kentli, A.; ÖzBeYAz, K.; Şahbaz, M.; Uçar, M. Investigation of strain inhomogeneity in hexa-ECAP processed AA7075. *Arch. Metall. Mater.* **2021**, *66*, 431–436. [\[CrossRef\]](#)

51. Eivani, A.R.; Rahimi, F. Inhomogeneity in deformation, microstructure, tensile properties and damage development in AA1050 during multiple cycles of pure shear extrusion. *Mater. Sci. Eng. A* **2019**, *745*, 159–167. [\[CrossRef\]](#)
52. Fatemi-Varzaneh, S.; Zarei-Hanzaki, A.; Vaghar, R.; Cabrera, J. The origin of microstructure inhomogeneity in Mg–3Al–1Zn processed by severe plastic deformation. *Mater. Sci. Eng. A* **2012**, *551*, 128–132. [\[CrossRef\]](#)
53. Basavaraj, V.P.; Chakkingal, U.; Kumar, T.P. Study of channel angle influence on material flow and strain inhomogeneity in equal channel angular pressing using 3D finite element simulation. *J. Mater. Process. Technol.* **2009**, *209*, 89–95. [\[CrossRef\]](#)
54. Bakhtiari, H.; Karimi, M.; Rezazadeh, S. Modeling, analysis and multi-objective optimization of twist extrusion process using predictive models and meta-heuristic approaches, based on finite element results. *J. Intell. Manuf.* **2016**, *27*, 463–473. [\[CrossRef\]](#)
55. Lotfan, S.; Ghiasi, R.A.; Fallah, M.; Sadeghi, M. ANN-based modeling and reducing dual-fuel engine's challenging emissions by multi-objective evolutionary algorithm NSGA-II. *Appl. Energy* **2016**, *175*, 91–99. [\[CrossRef\]](#)
56. Moré, J.J. The Levenberg-Marquardt algorithm: Implementation and theory. In *Numerical Analysis: Proceedings of the Biennial Conference Held at Dundee, Dundee, Scotland, 28 June–1 July 1977*; Springer: Berlin/Heidelberg, Germany; pp. 105–116.
57. Deb, K.; Pratap, A.; Agarwal, S.; Meyarivan, T. A fast and elitist multiobjective genetic algorithm: NSGA-II. *IEEE Trans. Evol. Comput.* **2002**, *6*, 182–197. [\[CrossRef\]](#)
58. Maganti, N.R.; Kumar, K.N. Effect of equal channel angular pressing process on the hardness and microstructure of copper and Al-6082 alloy: A preliminary investigation. *Mater. Today Proc.* **2017**, *4*, 8400–8408. [\[CrossRef\]](#)
59. El-Danaf, E.A. Mechanical properties, microstructure and texture of single pass equal channel angular pressed 1050, 5083, 6082 and 7010 aluminum alloys with different dies. *Mater. Des.* **2011**, *32*, 3838–3853. [\[CrossRef\]](#)
60. Özdoğan, E.F.; KAYALI, E.S. Eş kanallı açılal pres yöntemiyle üretilen Zr ve Sc ile modifiye edilmiş AA 6082 alüminyum alaşımının karakterizasyonu. *İtühderğıİ/D* **2011**, *10*, 99–106.
61. Dadbakhsh, S.; Taheri, A.K.; Smith, C. Strengthening study on 6082 Al alloy after combination of aging treatment and ECAP process. *Mater. Sci. Eng. A* **2010**, *527*, 4758–4766. [\[CrossRef\]](#)
62. Winter, L.; Hockauf, K.; Winter, S.; Lampke, T. Equal-channel angular pressing influencing the mean stress sensitivity in the high cycle fatigue regime of the 6082 aluminum alloy. *Mater. Sci. Eng. A* **2020**, *795*, 140014. [\[CrossRef\]](#)
63. Öğüt, S. Investigation on Mechanical Properties of Magnesium and Copper Alloys Processed by Expansion Equal Channel Angular Extrusion. Doctoral Thesis, Marmara Üniversitesi, İstanbul, Turkey, 2021.

Disclaimer/Publisher's Note: The statements, opinions and data contained in all publications are solely those of the individual author(s) and contributor(s) and not of MDPI and/or the editor(s). MDPI and/or the editor(s) disclaim responsibility for any injury to people or property resulting from any ideas, methods, instructions or products referred to in the content.